

# Infrared Emission of Specific Polycyclic Aromatic Hydrocarbon Molecules: Cyanonaphthalenes

DRAFT: 2024.3.11.117

Kaijun Li<sup>1</sup>, Aigen Li<sup>2</sup>, X.J. Yang<sup>3</sup>, and Taotao Fang<sup>1</sup>

## ABSTRACT

The unidentified infrared emission (UIE) features at 3.3, 6.2, 7.7, 8.6, 11.3 and 12.7  $\mu\text{m}$  are ubiquitously seen in a wide variety of astrophysical regions and commonly attributed to polycyclic aromatic hydrocarbon (PAH) molecules. However, the unambiguous identification of any individual, specific PAH molecules has proven elusive until very recently two isomers of cyanonaphthalene, which consists of two fused benzene rings and substitutes a nitrile ( $-\text{CN}$ ) group for a hydrogen atom, were discovered in the Taurus Molecular Cloud based on their rotational transitions at radio frequencies. To facilitate the *James Webb Space Telescope* (JWST) to search for cyanonaphthalenes in astrophysical regions, we model the vibrational excitation of cyanonaphthalenes and calculate their infrared emission spectra in a number of representative astrophysical regions. The model emission spectra and intensities will allow *JWST* to quantitatively determine or place an upper limit on the abundances of cyanonaphthalenes.

*Subject headings:* dust, extinction — ISM: lines and bands — ISM: molecules

## 1. Introduction

The “unidentified infrared emission” (UIE) bands, a distinct set of spectral features at wavelengths of 3.3, 6.2, 7.7, 8.6, 11.3 and 12.7  $\mu\text{m}$ , dominate the infrared (IR) spectra of many bright astronomical objects. They are ubiquitously seen in the interstellar medium (ISM) of our own galaxy and star-forming galaxies, both near (e.g., the Local Group) and far (e.g., distant galaxies at redshifts  $z > 4$ ), and account for up to 20% of their total infrared (IR) luminosity (see Li 2020). The identification of the UIE bands is important as they are a useful probe of the cosmic star-formation history, and their carriers are an essential player in galactic evolution. Although the exact nature of the UIE bands remains unknown, a popular hypothesis is that they arise from the

---

<sup>1</sup>Department of Astronomy, Xiamen University, Xiamen, Fujian 361005, China; fangt@xmu.edu.cn

<sup>2</sup>Department of Physics and Astronomy, University of Missouri, Columbia, MO 65211, USA; lia@missouri.edu

<sup>3</sup>Department of Physics, Xiangtan University, 411105 Xiangtan, Hunan Province, China; xjyang@xtu.edu.cn

C–H and C–C vibrational transitions of polycyclic aromatic hydrocarbon (PAH) molecules (Léger & Puget 1984, Allamandola et al. 1985, Tielens 2008).

Nevertheless, despite the popularity of the PAH hypothesis, unambiguous astronomical identification of any individual, specific PAH molecules has long proven elusive for nearly four decades ever since the PAH model was first proposed in the 1980s. However, recent years have witnessed breakthroughs in this aspect. Based on radio observations of the dark molecular cloud TMC-1 located within the Taurus Molecular Cloud made by the 100 m Green Bank Telescope (GBT) in the frequency range of 8 to 34 GHz, McGuire et al. (2021) reported the detection of the rotational transitions of 1-cyanonaphthalene (1-CNN) and 2-cyanonaphthalene (2-CNN), two isomers of cyanonaphthalene ( $C_{10}H_7CN$ ), in which a nitrile/cyano ( $-CN$ ) group replaces one of the hydrogen atoms of naphthalene (see Figure 1). This is the first definitive identification of a specific PAH molecule in space. Similarly, Burkhardt et al. (2021) conducted GBT radio observations of TMC-1 in the frequency range of 2–12 and 18–34 GHz. They detected indene ( $C_9H_8$ ), a pure hydrocarbon PAH species composed of both a five- and six-membered ring (see Figure 1).

Prior to these, benzene ( $C_6H_6$ ) was detected in CRL 618, a protoplanetary nebula, through a single weak absorption feature arising from its  $\nu_4$  bending mode at  $\sim 14.85 \mu m$  (Cernicharo et al. 2001). Recently, benzene has also been detected by the *James Webb Space Telescope* (JWST) through the  $14.85 \mu m$  emission feature in a protoplanetary disk around a low-mass star (Tabone et al. 2023). Benzonitrile ( $C_6H_5CN$ ), a single benzene ring with an attached CN group, was discovered also with GBT by McGuire et al. (2018) in TMC-1. This discovery was also achieved by radio observations of its rotational lines in the frequency range of 18 to 23 GHz. By definition, benzene and benzonitrile are aromatic but not PAH molecules. For illustration, Figure 1 lists all these specific aromatic species spectroscopically identified in space.<sup>1</sup> These aromatic molecules may be precursors to more complex PAHs. The identification of these specific aromatic molecules sheds light on the composition of aromatic material within the ISM that will eventually be incorporated into new stars and planets.

Nevertheless, identification of specific PAH molecules through IR spectroscopy has so far been ineffective. The UIE bands are attributed to collective emission from many different PAH species and thus do not allow one to fingerprint individual PAH molecules. However, the IR spectra of different PAH molecules are readily distinguishable in the laboratory from one species to another. Therefore, in principle, IR spectroscopy could provide individual identification if the molecule is sufficiently abundant and the telescope instrument is sufficiently sensitive. With the advent of JWST, this may become possible due to its unprecedented sensitivity. With an aim to offer spectroscopic

---

<sup>1</sup>Several small PAHs, including naphthalene ( $C_{10}H_8$ ), phenanthrene ( $C_{14}H_{10}$ ), perylene ( $C_{16}H_{10}$ ), pyrene ( $C_{20}H_{12}$ ), and their derivatives have been found in the *Stardust* samples collected from comet Wild 2 (Sandford et al. 2006, Clemett et al. 2010), in the *Rosetta* samples collected from comet 67P/Churyumov-Gerasimenko (Schuhmann et al. 2019), in the *Hayabusa 2* samples collected from the carbonaceous asteroid Ryugu (Naraoka et al. 2023), and in interplanetary dust particles possibly of cometary origin (Clemett et al. 1993). These PAH molecules were identified through mass spectrometry, not through vibrational or rotational spectroscopy.

guidance for JWST to search for specific PAH molecules, we perform a systematic exploration of the theoretical IR emission spectra of various specific PAH species expected in different astrophysical environments. In this work, we report the model IR emission spectra for cyanonaphthalenes (i.e., 1- and 2-CNN), the first PAH molecules ever detected in the ISM. In §2 we synthesize the ultraviolet (UV) absorption cross sections which determine how cyanonaphthalenes absorb starlight in space. The IR absorption cross sections are also discussed in §2 which determine how cyanonaphthalenes emit in the IR. The vibrational excitation and de-excitation of cyanonaphthalenes are discussed in §3. We present in §4 the model IR emission spectra of cyanonaphthalenes. The results are discussed in §5 and summarized in §6.

## 2. UV and IR Absorption Cross Sections

The UV absorption cross sections of cyanonaphthalenes determine how they absorb starlight photons in space. Unfortunately, the UV absorption has only been measured for 1-CNN over the wavelength range of  $0.21 \mu\text{m} < \lambda < 0.33 \mu\text{m}$  (Perkampus 1992). Therefore, for  $0.14 \mu\text{m} < \lambda < 0.21 \mu\text{m}$  we adopt the UV absorption of naphthalene (Robin 1975) and for  $0.04 \mu\text{m} < \lambda < 0.14 \mu\text{m}$  we take the vacuum UV absorption measured by Koch et al. (1972) for naphthalene. Finally, as shown in Figure 2, the UV absorption spectra of naphthalene are smoothly scaled to join that of 1-CNN. As cyanonaphthalenes are too small to absorb appreciably in the visible, for  $\lambda > 0.33 \mu\text{m}$  we therefore extrapolate from that of Perkampus (1992) at  $\lambda < 0.33 \mu\text{m}$ . Due to lack of experimental data, we do not distinguish the UV absorption between 1-CNN and 2-CNN.

In the IR, Bauschlicher (1998) have computed the vibrational frequencies and intensities of 1-CNN and 2-CNN, using the B3LYP density functional theory in conjunction with the 4-31G basis set. We take the vibrational frequencies and intensities of Bauschlicher (1998) which are available from the *NASA Ames PAH IR Spectroscopic Database* (Boersma et al. 2014, Bauschlicher et al. 2018, Mattioda et al. 2020). We represent each vibrational line by a Drude function,<sup>2</sup> characterized by the peak wavelength and intensity of the vibrational transition. In addition, we assign a width of  $30 \text{ cm}^{-1}$  for each line, consistent with the natural line width expected from a vibrationally excited PAH molecule (see Allamandola et al. 1999). The resulting IR absorption sections of 1-CNN and 2-CNN are shown in Figure 3. It is remarkable that the IR vibrational spectra of 1-CNN and 2-CNN are quite similar at  $\lambda < 10 \mu\text{m}$  and even at  $\lambda > 10 \mu\text{m}$  they do not differ substantially. This will be further discussed in §4.

---

<sup>2</sup>If we approximate the vibrational modes of PAHs as harmonic oscillators, the absorption cross sections are then expected to be Drude functions (see Li 2009).

### 3. Vibrational Excitation of Cyanonaphthalenes

Cyanonaphthalenes only have 19 atoms and 51 vibrational degrees of freedom. Upon absorption of an UV stellar photon, cyanonaphthalenes will undergo stochastic heating since their energy contents are often smaller than the energy of a single stellar photon. We model the stochastic heating of cyanonaphthalenes by employing the “exact-statistical” method of Draine & Li (2001). We characterize the state of a cyanonaphthalene molecule (i.e., 1-CNN or 2-CNN) by its vibrational energy  $E$ , and group its energy levels into  $(M + 1)$  “bins”, where the  $j$ -th bin ( $j = 0, \dots, M$ ) is  $[E_{j,\min}, E_{j,\max})$ , with representative energy  $E_j \equiv (E_{j,\min} + E_{j,\max})/2$ , and width  $\Delta E_j \equiv (E_{j,\max} - E_{j,\min})$ . Let  $P_j$  be the probability of finding 1-CNN (or 2-CNN) in bin  $j$  with energy  $E_j$ . The probability vector  $P_j$  evolves according to

$$dP_i/dt = \sum_{j \neq i} \mathbf{T}_{ij} P_j - \sum_{j \neq i} \mathbf{T}_{ji} P_i \quad , \quad i = 0, \dots, M \quad , \quad (1)$$

where the transition matrix element  $\mathbf{T}_{ij}$  is the probability per unit time for 1-CNN (or 2-CNN) in bin  $j$  to make a transition to one of the levels in bin  $i$ . We solve the steady state equations

$$\sum_{j \neq i} \mathbf{T}_{ij} P_j = \sum_{j \neq i} \mathbf{T}_{ji} P_i \quad , \quad i = 0, \dots, M \quad (2)$$

to obtain the  $M+1$  elements of  $P_j$ , and then calculate the resulting IR emission spectrum (see eq. 55 of Draine & Li 2001).

In calculating the state-to-state transition rates  $\mathbf{T}_{ji}$  for transitions  $i \rightarrow j$ , we distinguish the excitation rates  $\mathbf{T}_{ul}$  (from  $l$  to  $u$ ,  $l < u$ ) from the deexcitation rates  $\mathbf{T}_{lu}$  (from  $u$  to  $l$ ,  $l < u$ ). For a given starlight energy density  $u_E$ , the rates for upward transitions  $l \rightarrow u$  (i.e., the excitation rates) are just the photon absorption rates:

$$\mathbf{T}_{ul} \approx C_{\text{abs}}(E) c u_E \Delta E_u / (E_u - E_l) \quad . \quad (3)$$

The rates for downward transitions  $u \rightarrow l$  (i.e., the deexcitation rates) can be determined from the detailed balance analysis of the Einstein  $A$  coefficient:

$$\mathbf{T}_{lu} \approx \frac{8\pi}{h^3 c^2} \frac{g_l}{g_u} \frac{\Delta E_u}{E_u - E_l} E^3 \times C_{\text{abs}}(E) \left[ 1 + \frac{h^3 c^3}{8\pi E^3} u_E \right] \quad , \quad (4)$$

where  $h$  is the Planck constant, and the degeneracies  $g_u$  and  $g_l$  are the numbers of energy states in bins  $u$  and  $l$ , respectively:

$$g_j \equiv N(E_{j,\max}) - N(E_{j,\min}) \approx (dN/dE)_{E_j} \Delta E_j \quad , \quad (5)$$

where  $(dN/dE)_{E_j}$  is the vibrational density of states of 1-CNN (or 2-CNN) at internal energy  $E_j$ . For a cyanonaphthalene molecule, if we know the frequencies of all its 51 vibrational modes, we can employ the Beyer-Swinehart numerical algorithm (Beyer & Swinehart 1973, Stein & Rabinovitch

1973) to calculate the vibrational density of states  $(dN/dE)_{E_j}$  and therefore the degeneracies  $g_j$  for each vibrational energy bin. Meanwhile, if we know the oscillator strength of each vibrational mode, we can obtain the IR absorption cross section  $C_{\text{abs}}(E)$  by summing up all the vibrational transitions with each approximated as a Drude profile. Without a prior knowledge of the width of each vibrational transition, we assign a width of  $30 \text{ cm}^{-1}$ , consistent with the natural line width expected from free-flying molecule (see Allamandola et al. 1999). This natural line width arises from intramolecular vibrational energy redistribution.

As mentioned earlier (see §2), Bauschlicher (1998) have computed with B3LYP/4-31G the frequency and intensity for each of the 51 vibrational transitions of 1-CNN and 2-CNN. Therefore, we can calculate the vibrational density of states and the degeneracy  $g_j$  for each vibrational energy bin as well as the IR absorption cross section  $C_{\text{abs}}(E)$  by adopting the vibrational frequencies and intensities of 1-CNN and 2-CNN computed by Bauschlicher (1998). For a given astrophysical environment characterized by its starlight energy density  $u_E$ , we first calculate the excitation rates  $\mathbf{T}_{ul}$  (from  $l$  to  $u$ ,  $l < u$ ) according to eq. 3, using the UV absorption cross sections described in §2. We then calculate the deexcitation rates  $\mathbf{T}_{lu}$  (from  $u$  to  $l$ ,  $u > l$ ) according to eq. 4, using the degeneracy  $g_j$  and the IR absorption cross section  $C_{\text{abs}}(E)$  derived from the vibrational frequencies and intensities of Bauschlicher (1998). With the state-to-state transition rates  $\mathbf{T}_{ji}$  determined, we solve the steady-state probability evolution equation (see eq. 2) to obtain the steady-state energy probability distribution  $P_j$  and finally calculate the resulting IR emission spectrum, according to eq. 55 of Draine & Li (2001). For computational convenience, we consider 500 energy bins (i.e.,  $M = 500$ ).

#### 4. Model Emission Spectra

We first consider cyanonaphthalenes in the diffuse ISM excited by the solar neighborhood interstellar radiation field of Mathis et al. (1983; hereafter MMP83). Figure 4a shows the IR emissivities ( $\text{erg s}^{-1} \text{ sr}^{-1} \text{ cm}^{-1}$ ) per molecule for 1-CNN and 2-CNN. A first glance of Figure 4a reveals that the IR emission spectra of 1-CNN and 2-CNN are rather similar. Both exhibit a prominent C–H stretching band at  $3.26 \mu\text{m}$ , a prominent C–N stretching band at  $4.69 \mu\text{m}$ , and a broad complex at  $\sim 6\text{--}9 \mu\text{m}$  consisting of a number of sub-features arising from C–C stretching and C–H in-plane bending vibrations. The C–H out-of-plane bending bands at  $\sim 10.5\text{--}13.5 \mu\text{m}$  are also similar, except for 1-CNN they coalesce into a broad band at  $12.7 \mu\text{m}$ , while for 2-CNN several sub-features remain to be noticeable. The C-C-C skeletal bending band occurs at a longer wavelength for 1-CNN ( $\sim 22 \mu\text{m}$ ) compared to 2-CNN ( $\sim 21 \mu\text{m}$ ), otherwise they are also similar. Because of the close similarity between the emission spectra of 1-CNN and 2-CNN, in the following we will only consider 1-CNN.

To verify the single-photon heating nature of cyanonaphthalenes, we calculate the IR emission of 1-CNN excited by enhanced MMP83-type radiation fields. Figure 4b shows the IR emission spectra of 1-CNN excited by the MMP83 radiation field, but enhanced by a factor of  $U = 1000$  and

$10^5$  ( $U = 1$  corresponds to the MMP83 radiation field). As illustrated in Figure 4b, when scaled by  $U$ , the IR emission spectra are identical. This justifies the stochastic heating treatment of the vibrational excitation of cyanonaphthalenes. In the single-photon heating regime, the resulting IR emission is only dependent on the energy of the illuminating starlight photons, not on the starlight intensity.

We also examine how the IR emission of cyanonaphthalenes depends on the starlight spectrum (i.e., the “hardness” of the exciting radiation field). To this end, we consider 1-CNN exposed to stars with different effective temperatures:  $T_{\text{eff}} = 40,000, 22,000, 8,000$  K. The starlight spectra are approximated by the Kurucz model atmospheric spectra. Figure 5a shows the IR emission of 1-CNN illuminated by stars of  $T_{\text{eff}} = 40,000$  K (like O6V stars) with an intensity of  $U = 10^4$ , where  $U$  is defined as

$$U = \frac{\int_{1\mu\text{m}}^{912\text{\AA}} 4\pi J_{\star}(\lambda, T_{\text{eff}}) d\lambda}{\int_{1\mu\text{m}}^{912\text{\AA}} 4\pi J_{\text{ISRF}}(\lambda) d\lambda}, \quad (6)$$

where  $J_{\text{ISRF}}(\lambda)$  is the MMP83 radiation intensity, and  $J_{\star}(\lambda, T_{\text{eff}})$  is the intensity of starlight approximated by the Kurucz model atmospheric spectrum. Such a starlight spectrum and intensity resemble that of the Orion Bar photodissociation region and the M17 star-forming region. A comparison of Figure 5a with Figure 4b reveals that the IR emission spectra are almost identical for 1-CNN excited by the MMP83 field and by stars of  $T_{\text{eff}} = 40,000$  K, except the emissivity level is higher for the latter since the mean absorbed photon energy is higher for the latter.

Figure 5b shows the IR emission of 1-CNN illuminated by stars of  $T_{\text{eff}} = 22,000$  K (like B1.5V stars) with an intensity of  $U = 10^3$ . This would be the case if 1-CNN is located in the reflection nebula NGC 2023. If scaled by  $U$  and the mean absorbed photon energy, the IR emission spectrum for  $T_{\text{eff}} = 22,000$  K is essentially identical to that for  $T_{\text{eff}} = 40,000$  K.

Figure 5c shows the IR emission of 1-CNN illuminated by stars of  $T_{\text{eff}} = 8,000$  K (like A5V stars) with an intensity of  $U = 10^5$ . The Red Rectangle protoplanetary nebula is illuminated by such a starlight spectrum and intensity.<sup>3</sup> Cyanonaphthalenes in the Red Rectangle would be excited by stellar photons much softer than that in the Orion Bar. It is therefore not unexpected that, as illustrated in Figure 5c, 1-CNN in the Red Rectangle would emit somewhat more at longer wavelengths compared to that in the Orion Bar. Nevertheless, the overall spectral shape does not differ considerably between that of the Red Rectangle and that of the Orion Bar.

Finally, we also consider the TMC-1 molecular cloud where cyanonaphthalenes were first detected through their rotational lines. The TMC-1 cloud is externally illuminated by the general interstellar radiation field and has a total visual extinction of  $\sim 3.6$  mag (Whittet et al. 2004). Therefore, to calculate the IR emission of cyanonaphthalenes in the TMC-1 cloud, we take the

---

<sup>3</sup>It is worth noting that Witt et al. (2009) argued that the Red Rectangle protoplanetary nebula is illuminated by a binary, and the UV radiation in this nebula does not come from HD 44179 of which  $T_{\text{eff}} \approx 8,000$  K, but rather from the accretion disk surrounding the secondary star in this binary, with  $T_{\text{eff}}$  in the range of  $\sim 17,000$ – $25,000$  K.

MMP83 interstellar radiation field, but attenuated by dust extinction with  $A_V = 1.8$  mag (from the cloud surface to the cloud core) and a wavelength-dependence  $A_\lambda/A_V$  like that of the Galactic average extinction curve of  $R_V = 3.1$ , where  $R_V$  is the total-to-selective extinction ratio (see Cardelli et al. 1989), i.e., cyanonaphthalenes in the TMC-1 cloud are assumed to be excited by starlight with an intensity of  $J_{\text{ISRF}}(\lambda) \times \exp\{-(A_V/1.086) \times (A_\lambda/A_V)\}$ . Figure 5d shows the IR emission of 1-CNN calculated for the TMC-1 cloud. Compared to that excited by the MMP83 radiation field (see Figure 4b), the overall IR emission spectrum of 1-CNN expected in the TMC-1 cloud is closely similar, except the emissivity level is appreciably reduced and the  $3.26 \mu\text{m}$  C–H stretch and  $4.69 \mu\text{m}$  C–N stretch emit slightly less.

## 5. Discussion

It is gratifying that, as illustrated in Figure 5a–d, the IR emission spectra of cyanonaphthalenes are not sensitive to the illuminating starlight spectrum. This is because, as shown in Figure 6, due to their small heat contents, the energy probability distribution functions of cyanonaphthalenes closely resemble each other, upon excited by starlight of different intensities and different spectral shapes.

While observationally the identification of cyanonaphthalenes through the  $\sim 6\text{--}9 \mu\text{m}$  complex and the  $10.5\text{--}13.5 \mu\text{m}$  complex could be complicated by the  $6.2$ ,  $7.7$ ,  $8.6$ ,  $11.3$  and  $12.7 \mu\text{m}$  UIE bands, the detection of the  $3.26$  and  $4.69 \mu\text{m}$  bands, and, to a less degree, the  $21$  or  $22 \mu\text{m}$  band, could *potentially* allow one to identify cyanonaphthalenes in space. Prior to JWST, the detection and identification of the spectral features as possibly due to cyanonaphthalenes would have been hampered by their small intensities which would put them at the limit of modern observational techniques, including the *Short Wavelength Spectrometer* (SWS) on board the *Infrared Space Observatory* (ISO) and the *Infrared Camera* (IRC) on board *AKARI*. With the advent of JWST, this will change. The *Near InfraRed Spectrograph* (NIRSpec) and *Mid-Infrared Instrument* (MIRI) on *JWST* span the wavelength range of the characteristic vibrational bands of cyanonaphthalenes. *JWST*'s unique high sensitivity and high resolution capabilities will open up an IR window unexplored by *Spitzer*<sup>4</sup> and unmatched by *ISO* observations and thus could potentially place the detection of the IR vibrational bands of individual PAH molecules on firm ground.

Admittedly, it is not clear if the detection of the  $3.26 \mu\text{m}$  C–H and  $4.69 \mu\text{m}$  C–N stretching bands could *uniquely* pinpoint the presence of cyanonaphthalenes, as other cyano-substituted PAHs may also emit at similar wavelengths. Note that cyano-benzene (benzonitrile) and cyano-indene have also been detected in TMC-1 (McGuire et al. 2018, Sita et al. 2022). To this end, a systematic calculation of the IR emission spectra of these molecules would be crucial. One can imagine that

---

<sup>4</sup>The *Infrared Spectrograph* (IRS) on *Spitzer* only operates longward of  $\sim 5.2 \mu\text{m}$  and does not cover the characteristic  $3.26 \mu\text{m}$  C–H and  $4.69 \mu\text{m}$  C–N stretching bands of cyanonaphthalenes.

different-sized cyano-containing aromatic molecules would exhibit different C–H/C–N band ratios since, with different energy contents, they are expected to be excited to different energy levels by the same stellar photon.

Let  $N_{\text{H}}$  be the hydrogen column density along the line of sight to an astrophysical region. Let  $[\text{C}/\text{H}]_{\text{CNN}}$  be the number of carbon atoms (per H nucleon) locked up in a cyanonaphthalene molecule. The intensity of the IR emission ( $\text{erg s}^{-1} \text{cm}^{-3} \text{sr}^{-1}$ ) expected from cyanonaphthalenes would be

$$I_{\lambda} = j_{\lambda} \times \left( \frac{N_{\text{H}}}{11} \right) \times \left[ \frac{\text{C}}{\text{H}} \right]_{\text{CNN}} , \quad (7)$$

where the denominator “11” accounts for the fact that a cyanonaphthalene molecule has 11 carbon atoms. The column density of cyanonaphthalenes is simply

$$N_{\text{CNN}} = \left( \frac{N_{\text{H}}}{11} \right) \times \left[ \frac{\text{C}}{\text{H}} \right]_{\text{CNN}} . \quad (8)$$

Therefore, by comparing the observed intensity  $I_{\lambda}^{\text{obs}}$  with the model emissivity  $j_{\lambda}$  (e.g., see Figure 5a–d), one can derive  $N_{\text{CNN}}$ . If  $N_{\text{H}}$  is known, then one can determine how much carbon is locked up in cyanonaphthalenes. On the other hand, if  $N_{\text{CNN}}$  is known (e.g., for 1-CNN or 2-CNN in TMC-1 from the measurements of their rotational lines), one can predict the IR emission intensity  $I_{\lambda}$  by multiplying the model emissivity shown in Figure 5a–d with  $N_{\text{CNN}}$ .

While cyanonaphthalenes are present in the UV-attenuated TMC-1 molecular cloud, it is not clear if they can survive in hostile regions where the UV radiation is intense (e.g., the diffuse ISM, the Orion Bar and the M17 star-forming cloud). According to Jacovella et al. (2022), HCN removal from protonated benzonitrile requires only  $\sim 3.4 \text{ eV}$ . As similar HCN removal energies are expected for cyanonaphthalenes, the survivability of these species in UV-irradiated environments such as the Orion Bar is questionable. It has been argued that only PAHs with more than 20 carbon atoms may survive in these regions (see Tielens 2008). However, Stockett et al. (2023) recently found that cyanonaphthalene can be efficiently stabilized following ionization, with the aid of the so-called “Recurrent Fluorescence” (also known as Poincaré fluorescence, see Léger et al. 1988), a radiative relaxation channel in which optical photons are emitted from thermally populated electronically excited states. Iida et al. (2022) also found that the Recurrent Fluorescence could efficiently stabilize small cationic carbon clusters with as few as nine carbon atoms. The Recurrent Fluorescence of PAHs excited by UV photons could reach high quantum efficiencies in photon conversion and has been suggested as the source of the so-called “extended red emission” (ERE; Witt & Lai 2020).

If the Recurrent Fluorescence does occur, the absorbed stellar photon energy will not be completely released through vibrational transitions. Therefore, the IR vibrational emissivity is expected to be somewhat lower than that calculated in Figure 5a–d, roughly by a factor of  $\langle h\nu \rangle_{\text{RF}} / \langle h\nu \rangle_{\text{abs}}$ , where  $\langle h\nu \rangle_{\text{RF}}$  is the mean energy of the optical photons emitted due to Recurrent Fluorescence, and  $\langle h\nu \rangle_{\text{abs}}$  is the mean energy of the absorbed stellar photons. For cyanonaphthalenes in the diffuse ISM, the reflection nebula NGC 7023, and the Orion Bar,  $\langle h\nu \rangle_{\text{abs}}$  is in the order of 8–9 eV. With



$\langle h\nu \rangle_{\text{RF}} \approx 2 \text{ eV}$  (see Stockett et al. 2023), the IR emissivity  $j_\lambda$  will only be reduced by  $\sim 20\%$  and the emission spectral profile will largely remain the same.

Finally, we note that the UV absorption cross sections of cyanonaphthalenes (i.e., 1-CNN and 2-CNN) adopted in this work were “synthesized” from 1-CNN and naphthalene (see §2). It is not clear how different the actual UV absorption cross sections of 1-CNN would be compared with naphthalene and of 2-CNN compared with 1-CNN. As a priori, one would imagine that the incorporation of a CN group in naphthalene, the parental molecule of cyanonaphthalenes, would cause significant changes to the UV absorption spectrum, as the  $\pi$  electrons of the CN group are partially conjugated with the main aromatic  $\pi$  system. Nevertheless, as mentioned earlier (see Figure 5a–d), the IR emission spectra of cyanonaphthalenes are not sensitive to the illuminating starlight spectrum. This also implies that the IR emission spectral shape of cyanonaphthalenes is not very sensitive to the exact UV absorption. In any case, future experimental measurements of the absorption spectra of cyanonaphthalenes from the optical to the far-UV will be helpful in examining their vibrational excitation.

We also note that the IR vibrational frequencies and intensities of cyanonaphthalenes adopted here were computed by Bauschlicher (1998), using a DFT force field and intensities in the harmonic limit. It is well recognized that anharmonic interactions could appreciably affect the vibrational frequencies and intensities. In addition, Fermi interactions can have a significant impact on the C–H stretches. Moreover, quadratic dipole dependence can also affect the vibrational intensities. While some of these effects could be grossly accounted for by empirical scaling coefficients as applied by Bauschlicher (1998), more accurate results may be obtained with the standard second-order vibrational perturbation theory (VPT2). Note that the VPT2 theory is feasible with DFT force fields for molecules as large as cyanonaphthalenes. Future quantum chemical computations utilizing the VPT2 theory and even better, experimental measurements of gas-phase cyanonaphthalenes will be helpful in evaluating the accuracy of the IR emission spectra calculated here.

In calculating the IR emission spectra of cyanonaphthalenes, we assume a natural line width of  $\gamma = 30 \text{ cm}^{-1}$  for each vibrational transition (see §2) due to internal vibration redistribution (IVR). This may be somewhat simplified. Molecules like cyanonaphthalenes are in a somewhat intermediate size-range, where IVR is prevalent, but not necessarily ergodic or completely statistical. For these molecules, spectral broadening may more likely be dominated by anharmonic shifts of the thermally excited vibrational levels. Indeed, Hewett et al. (1994) argued that the C–H fundamentals of naphthalene are far from the IVR threshold. In view of these, we have also considered  $\gamma = 10 \text{ cm}^{-1}$  and  $50 \text{ cm}^{-1}$ . As shown in Figure 7, the model IR emission spectra are essentially the same, particularly in the characteristic C–H and C–N stretching regions. This justifies the choice of a natural line width of  $\gamma = 30 \text{ cm}^{-1}$ .

## 6. Summary

We have modeled the vibrational excitation of cyanonaphthalenes, the first specific PAH species ever identified in space, and have calculated their IR emission spectra for a number of representative astrophysical regions, from the diffuse ISM to regions illuminated by stars of different effective temperatures. Also calculated includes the TMC-1 dark molecular cloud where cyanonaphthalenes were first detected through their rotational lines. It is found that while the emissivity level varies from one region to another, the overall IR emission spectra do not vary much with environments or between two isomers of cyanonaphthalene (i.e., 1-CNN and 2-CNN). Both isomers exhibit prominent bands at  $3.26\ \mu\text{m}$  (C–H stretch),  $4.69\ \mu\text{m}$  (C–N stretch), 21 or  $22\ \mu\text{m}$  (skeletal bend), and broad complexes at  $\sim 6\text{--}9\ \mu\text{m}$  and  $\sim 10.5\text{--}13.5\ \mu\text{m}$ . The NIRSpec and MIRI instruments on board JWST are well suited for searching for cyanonaphthalenes in space, particularly through the characteristic bands at  $3.26$  and  $4.69\ \mu\text{m}$ .

We thank the anonymous referees for helpful comments and suggestions. We thank B.M. Broderick, B.T. Draine, B.A. McGuire, and E.F. van Dishoeck for stimulating discussions. KJL and TTF are supported by the National Key R&D Program of China under No. 2017YFA0402600, and the NSFC grants 11890692, 12133008, and 12221003, as well as CMS-CSST-2021-A04. XJY is supported in part by NSFC 12333005 and 12122302 and CMS-CSST-2021-A09.

## REFERENCES

- Allamandola, L.J., Tielens, A.G.G.M., & Barker, J.R. 1985, *ApJ*, 290, L25
- Allamandola, L.J., Hudgins, D.M., & Sandford, S.A. 1999, *ApJ*, 511, 115
- Bauschlicher, C.W. 1998, *Chem. Phys.*, 234, 87
- Bauschlicher, C. W., Ricca, A., Boersma, C., & Allamandola, L.J. 2018, *ApJS*, 234, 32
- Beyer, T., & Swinehart, D.F. 1973, *Commun. Assoc. Comput. Machinery*, 16, 379
- Boersma, C., Bauschlicher, C.W., Ricca, A., et al. 2014, *ApJS*, 211, 8
- Burkhardt, A. M., Lee, K.L.K., Changala, P.B., et al. 2021, *ApJL*, 913, L18
- Cardelli, J. A., Clayton, G. C., & Mathis, J. S. 1989, *ApJ*, 354, 245
- Cernicharo, J., Heras, A. M., Tielens, A. G. G. M., et al. 2001, *ApJL*, 546, L123
- Clemett, S.J., Maechling, C.R., Zare, R.N., Swan, P.D., & Walker, R.M. 1993, *Science*, 262, 721
- Clemett, S. J., Sandford, S. A., Nakamura-Messenger, K., Hörz, F., & McKay, D.S. 2010, *Meteorit. Planet. Sci.*, 45, 701

- Draine, B.T., & Li, A. 2001, *ApJ*, 551, 807
- Hewett, K. B., Shen, M., Brummel, C. L., et al. 1994, *J. Chem. Phys.*, 100, 4077.
- Iida, S., Hu, W., Zhang, R., et al. 2022, *MNRAS*, 514, 844
- Jacovella, U., Noble, J. A., Guliani, A., et al. 2022, *A&A*, 657, A85
- Koch, E.E., Otto, A., & Radler, K. 1972, *Chem. Phys. Lett.*, 16, 131
- Léger, A., & Puget, J. 1984, *A&A*, 137, L5
- Léger, A., Boissel, & d'Hendecourt, L.B. 1988, *Phys. Rev. Lett.*, 60, 921
- Li, A. 2009, *Optical Properties of Dust*, in *Small Bodies in Planetary Sciences*, ed. I. Mann, A. Nakamura, & T. Mukai, Springer, 167
- Li, A. 2020, *Nature Astronomy*, 4, 339
- Mathis, J.S., Mezger, P.G., & Panagia, N. 1983, *A&A*, 128, 212
- Mattioda, A.L., Hudgins, D.M., Boersma, C., et al. 2020, *ApJS*, 251, 22
- McGuire, B. A., Burkhardt, A. M., Kalenskii, S., et al. 2018, *Science*, 359, 202
- McGuire, B. A., Loomis, R. A., Burkhardt, A. M., et al. 2021, *Science*, 371, 1265
- Naraoka, H., Takano, Y., Dworkin, J.P., et al. 2023, *Science*, 379, 9033
- Perkampus, H.H. 1992, *UV-VIS Atlas of Organic Compounds (2nd ed.)*, VCH, Weinheim
- Robin, M.B. 1975, *Higher Excited States of Polyatomic Molecules*, Vol. II (London: Academic Press)
- Sandford, S.A., Aléon, J., Alexander, C.M.O.D., et al. 2006, *Science*, 314, 1720
- Schuhmann, M., Altwegg, K., Balsiger, H., et al. 2019, *A&A*, 630, A31
- Sita, M. L., Changala, P. B., Xue, C., et al. 2022, *ApJL*, 938, L12
- Stein, S.E., & Rabinovitch, B.S. 1973, *J. Chem. Phys.*, 58, 2438
- Stockett, M. H., Bull, J. N., Cederquist, H., et al. 2023, *Nature Communications*, 14, 395
- Tabone, B., Bettoni, G., van Dishoeck, E.F., et al. 2023, *Nature Astronomy*, 7, 805
- Tielens, A. G. G. M. 2008, *ARA&A*, 46, 289
- Whittet, D. C. B., Shenoy, S. S., Clayton, G. C., & Gordon, K.D. 2004, *ApJ*, 602, 291

Witt, A. N., Vijh, U. P., Hobbs, L. M., Aufdenberg, J.P., Thorburn, J.A., & York, D.G. 2009, ApJ, 693, 1946

Witt, A. N., & Lai, T. S.-Y. 2020, Ap&SS, 365, 58

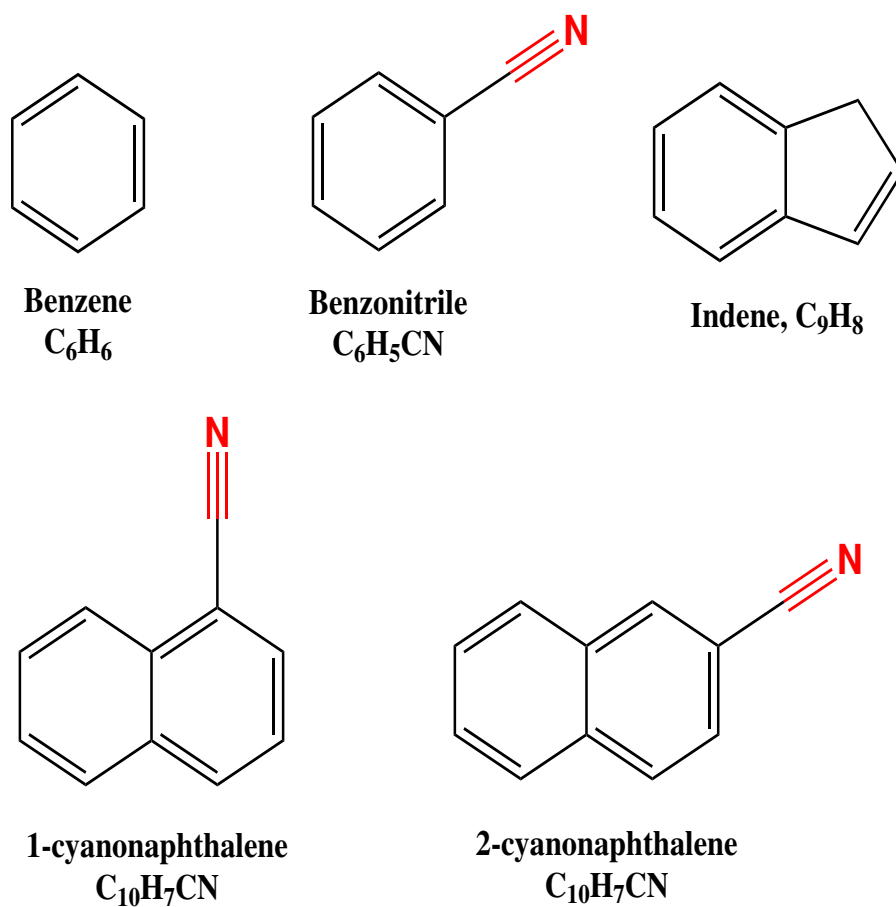


Fig. 1.— Chemical structures of specific aromatic molecules identified in the ISM.

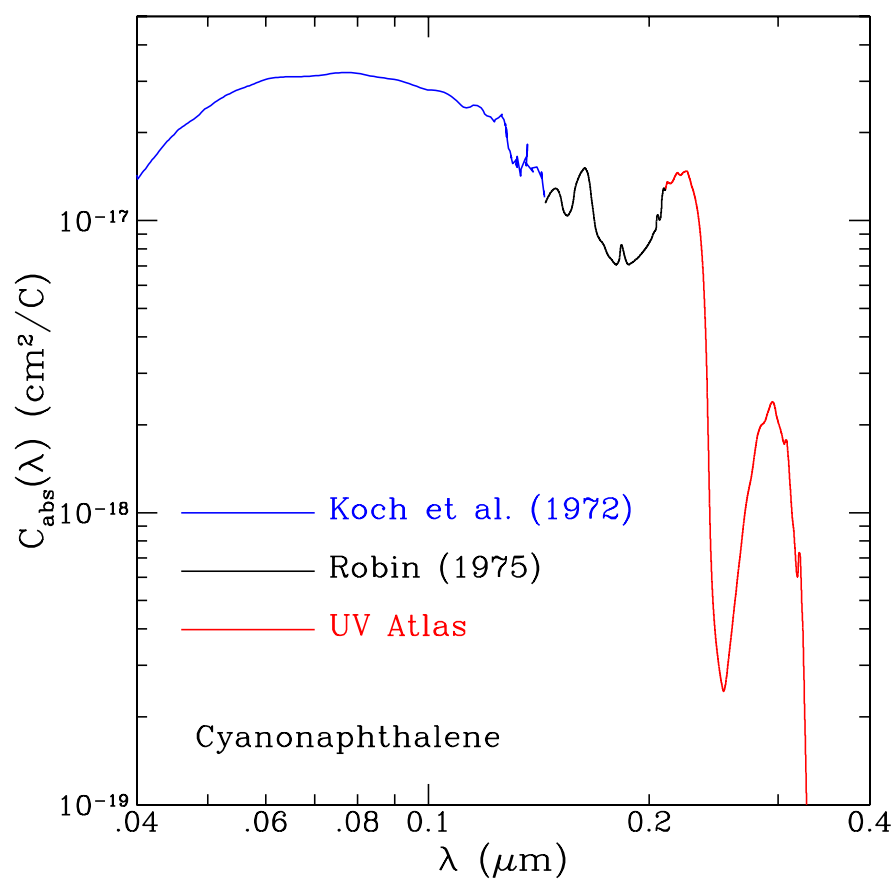


Fig. 2.— UV absorption cross sections (per C atom) of cyanonaphthalenes “synthesized” from the experimental data of 1-CNN over  $0.21 \mu\text{m} < \lambda < 0.33 \mu\text{m}$  (red line; Perkampus 1992), and of naphthalene over  $0.14 \mu\text{m} < \lambda < 0.21 \mu\text{m}$  (black line; Robin 1975) and over  $0.04 \mu\text{m} < \lambda < 0.14 \mu\text{m}$  (blue line; Koch et al. 1972).

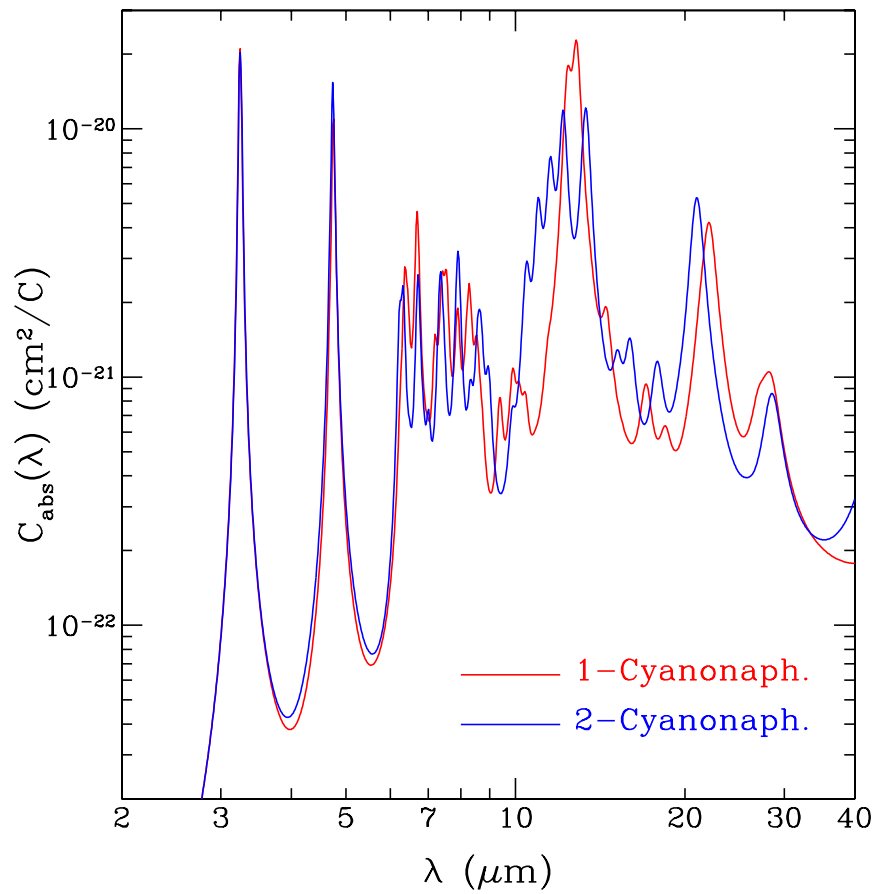


Fig. 3.— IR absorption cross sections (per C atom) of cyanonaphthalenes (red line: 1-CNN; blue line: 2-CNN) calculated from the vibrational frequencies and intensities computed by Bauschlicher (1998) using B3LYP/4-31G. Each vibrational line is assigned a width of  $30 \text{ cm}^{-1}$ , consistent with the natural line width expected from a vibrationally excited PAH molecule (see Allamandola et al. 1999).

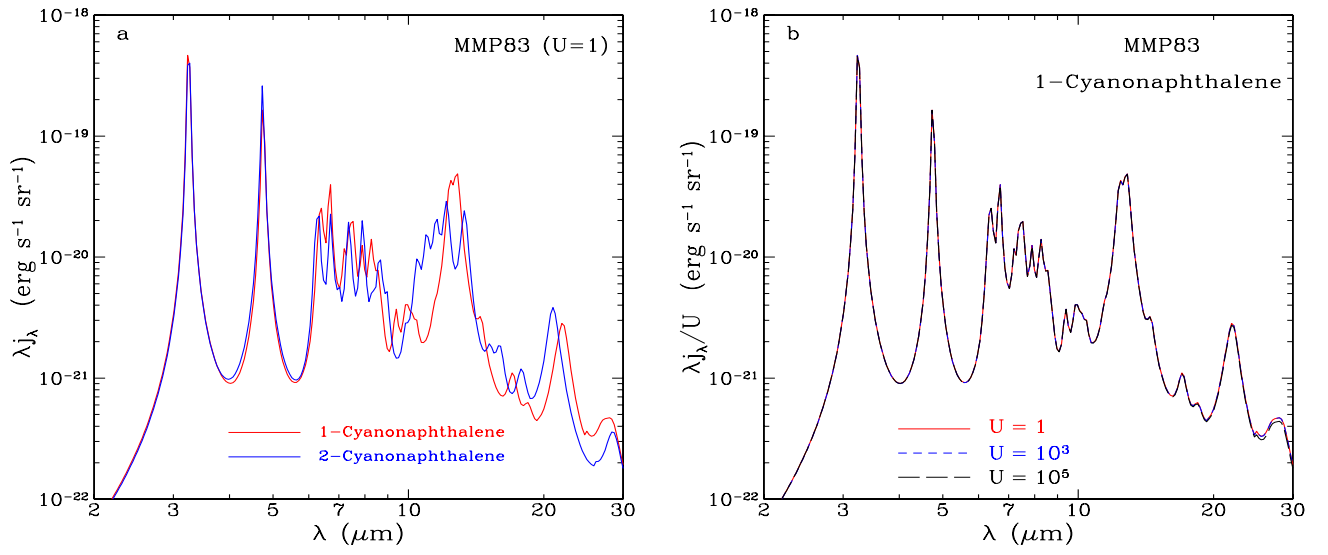


Fig. 4.— Left panel (a): IR emission spectra of 1-CNN (red line) and 2-CNN (blue line) illuminated by the MMP83 ( $U=1$ ) interstellar radiation field. Right panel (b): IR emission spectra of 1-CNN illuminated by the MMP83 radiation field with different intensities (red solid line:  $U=1$ ; blue shot-dashed line:  $U=1,000$ ; black long-dashed line:  $U=10^5$ ).

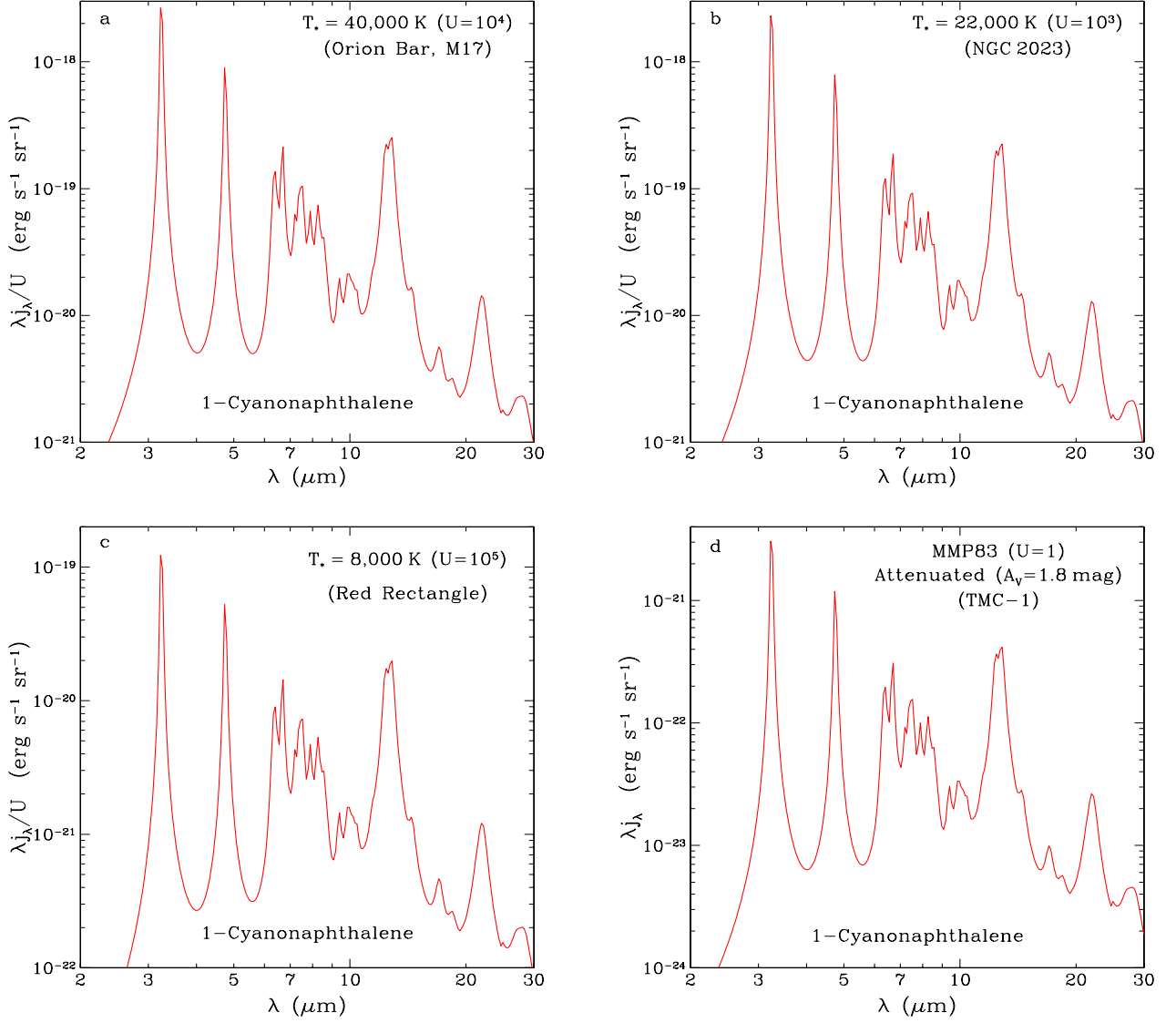


Fig. 5.— IR emission spectra of 1-CNN illuminated by radiation fields of different starlight spectra:  $T_{\text{eff}} = 40,000$  K and  $U = 10^4$  (top left panel, a),  $T_{\text{eff}} = 22,000$  K and  $U = 10^4$  (top right panel, b),  $T_{\text{eff}} = 8,000$  K and  $U = 10^5$  (bottom left panel, c), and MMP83 radiation field attenuated by a visual extinction of  $A_V = 1.8$  mag (bottom right panel, d).



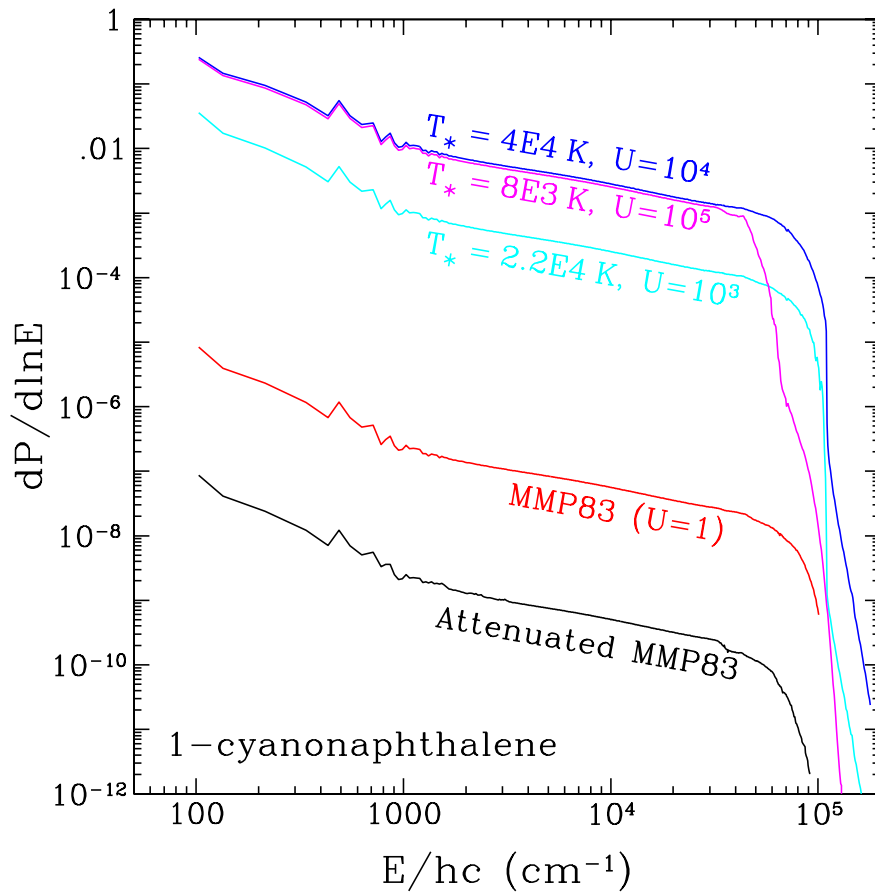


Fig. 6.— Vibrational energy probability distribution functions for the excited vibrational states of 1-CNN, exposed to radiation fields of different intensities ( $U$ ) and different spectral shapes: MMP83 (red), attenuated MMP83 (black), and stars of different effective temperatures (blue:  $T_{\text{eff}} = 4 \times 10^4$  K and  $U = 10^4$ , cyan:  $T_{\text{eff}} = 2.2 \times 10^4$  K and  $U = 10^3$ , and magenta:  $T_{\text{eff}} = 8 \times 10^3$  K and  $U = 10^5$ ).

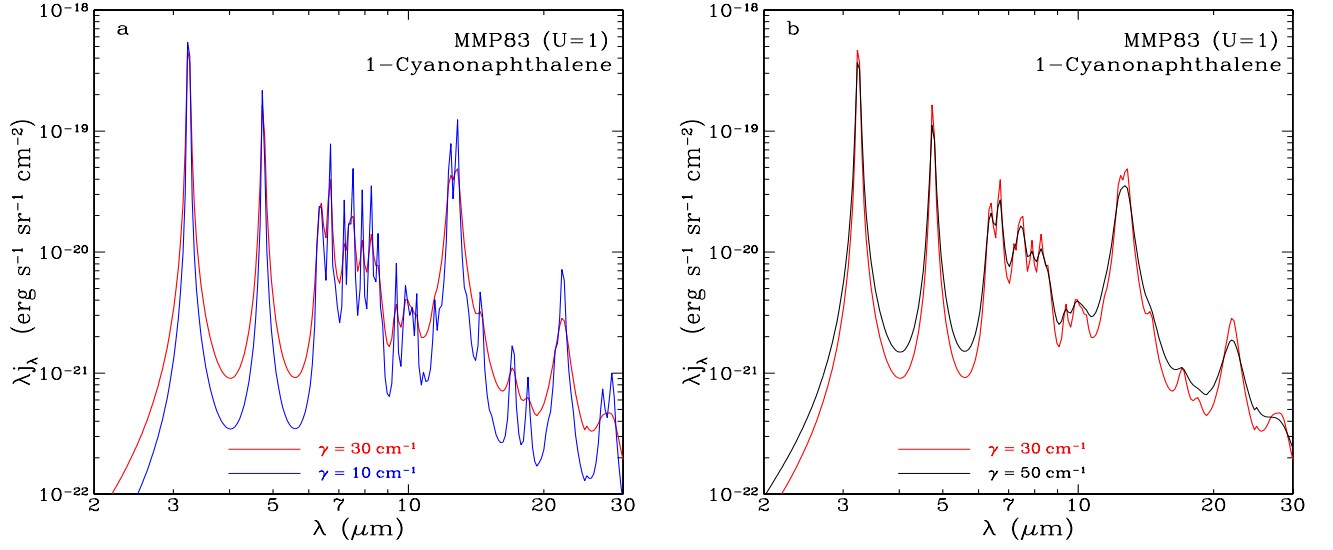


Fig. 7.— Left panel (a): Comparison of the IR emission spectra of 1-CNN of a natural line width of  $\gamma = 30 \text{ cm}^{-1}$  (red line) for each vibrational transition with that of  $\gamma = 10 \text{ cm}^{-1}$  (blue line). The molecule is illuminated by the MMP83 ( $U=1$ ) interstellar radiation field. Right panel (b): Same as (a) but for a comparison of  $\gamma = 30 \text{ cm}^{-1}$  (red line) with  $\gamma = 50 \text{ cm}^{-1}$  (blue line).